RADIO CONTINUUM STRUCTURE OF THE ORION NEBULA

RAVI SUBRAHMANYAN
Australia Telescope National Facility, CSIRO, Locked Bag 194, Narrabri, NSW 2390, Australia

W. M. GOSS
National Radio Astronomy Observatory, P.O. Box O, Socorro, NM 87801

AND

DAVID F. MALIN
Anglo-Australian Observatory, P.O. Box 296, Epping, NSW 1710, Australia

ABSTRACT

We have imaged the large-scale radio continuum structure in the Orion region with the Very Large Array at 330 MHz. Arcminute-resolution morphology of the extended emission in the H II regions M42 and M43 (NGC 1976 and NGC 1982) and in the NGC 1973-75-77 nebulosity to the north are presented. A low surface brightness thermal radio halo is detected in the H II region M42: comparison with an optical photograph indicates that the radio emission distinguishes optical emission structures from reflection nebulosities. In NGC 1977 we have discovered a compact, steep-spectrum radio source coincident with a bright optical rim.

Key words: H II regions — ISM: individual (NGC 1976, NGC 1977) — radio continuum — reflection nebulae

1. INTRODUCTION

Lockman (1980) suggested that centimeter-wavelength recombination lines, ubiquitous below 50° Galactic latitudes, probably originate in extended outer parts of normal H II regions. Anantharamaiah (1985) observed H272α radio recombination lines along the Galactic ridge in a survey conducted with the Ooty radio telescope: these may be produced only by low-density ionized gas, and Anantharamaiah (1986) suggests—after combining his results with previous high-frequency recombination line, continuum, and pulsar dispersion observations—that they originate in extended low-density envelopes of H II regions. More recently, Roshi & Anantharamaiah (2000) associated their detections of diffuse radio recombination lines toward the inner Galaxy with a low-density component of known H II regions. Detection of low-frequency turnovers in the radio spectra of Galactic supernova remnants has been interpreted as further evidence for the existence of extended H II region envelopes (Kassim 1989). The low filling factor derived for this component of the interstellar medium (ISM) led to the inference that these regions have an electron temperature $T_e \sim 3000$–8000 K, an electron density $n_e \sim$ 0.5–10.0 cm^{-3}, and sizes of 50–200 pc: these low-density envelopes are believed to surround the high-density "classical" H II regions.

The warm ionized medium, which has been estimated to have a similar temperature but a much lower density of $n_e \sim 0.3$ cm^{-3} (Kulkarni & Heiles 1987), may have a much larger filling factor in the ISM. The envelopes hypothesized as associated with H II regions may represent a spatial transition zone between the higher density H II regions and the warm ionized medium.

Smith, Biermann, & Mezger (1978) and Mezger (1978) have postulated that "classical" H II regions have short lifetimes relative to the OB associations that create them. Their picture is one in which the H II regions expand and evolve into extended low-density ionized gas that has a significant filling factor in the ISM, and this region was suggested as absorbing most of the ionizing photons in the Galaxy. However, more recently McKee & Williams (1997) construct a luminosity function for OB associations in our Galaxy and conclude that the radio H II regions and their associated H II envelopes absorb almost all the ionizing photons emitted in the Galaxy.

The Great Orion Nebula (NGC 1976, M42) is perhaps the most studied H II region (observations up to 1980 are summarized in Goudis 1982). More recent radio continuum images of the large-scale structure of the nebula include the 330 MHz VLA image (Subrahmanyan 1992) and the 1.4 GHz VLA image (Yusef-Zadeh 1990). Along with the 408 MHz image made by Mills & Shaver (1968), these images have detected extended emission surrounding the bright central H II region. When compared with the broadband Hα + [N II] image of the nebula published by Murdin, Allen, & Malin (1979) and other optical photographs, it appears that the radio emission has not been detected throughout the optical nebula. The fainter outer filamentary parts, particularly toward the south of the central peak, are detected in optical line and continuum but not in the radio: this has led to speculation that the outer parts of the optical halo may be the result of reflection from dust grains rather than emission from thermal bremsstrahlung (Peimbert 1982; Van der Werf & Goss 1989).

The total radio spectrum of M42 (reproduced in Goudis 1982) shows a low-frequency turnover below about 1 GHz; however, at low frequencies below about 100 MHz, the measurements indicate an upturn. The low-frequency measurements have been made with broad beams and may suffer from confusion; on the other hand, these measurements may be detecting a nonthermal halo component.

We have revisited the problem of whether or not extended thermal envelopes or halos exist around H II regions and look specifically for a halo in M42 in the radio continuum. We have imaged the VLA 330 MHz data (of Subrahmanyan 1992) using new imaging algorithms that better reproduce extended structure over wide fields and

have detected a radio halo enveloping M42. In § 2, we present the improved 330 MHz image of the Orion region. In §§ 3 and 4, we compare with a 1.5 GHz VLA image made by Yusef-Zadeh (1990) and a 10.55 GHz image of M42 and M43 made by us with the Effelsberg telescope. Section 5 discusses the implications for the extent and nature of the halo emission around the Orion Nebula.

Our new, wide-field image of the Orion region includes the NGC 1977 nebulosity to the north. Kutner et al. (1985) detected a peak in the 6 cm radio continuum image of this region that was coincident with a bright rim seen in optical images of the nebula. In § 6 we present our 330 MHz observations of this nebula and report our finding that the peak in continuum emission is a compact, steep-spectrum source.

2. 330 MHz VLA IMAGE OF THE ORION REGION

The Very Large Array (VLA; Napier, Thompson, & Ekers 1983) observations were described in Subrahmanyan (1992). In brief, the 330 MHz data were obtained in the DnC hybrid (3.5 hr integration time) and D array (4.3 hr); the visibility data obtained were distributed over ± 5 hr in hour angle. The absolute flux density calibration is believed to be accurate to within $\pm 4\%$.

Subrahmanyan (1992) imaged the data using the AIPS MX routine, which assumes a two-dimensional transform from the visibility domain to sky. The resulting imaging errors increase with distance from the image phase center. In addition, the point-spread function is increasingly inapplicable away from the phase center, resulting in deconvolution errors. Consequently, the arcminute-resolution image presented in Subrahmanyan (1992) covered only the H II regions M42 and M43 and had an rms noise of about 10 mJy beam^{-1}; the lowest reliable contour was plotted at 32 mJy beam^{-1}.

We have used these visibility data to construct a wide-field image of the Orion region. In contrast to Subrahmanyan (1992), we have used the three-dimensional imaging routine DRAGON in SDE implemented by T. J. Cornwell. This algorithm approximates the celestial sphere using polyhedral facets and avoids the imaging and deconvolution errors mentioned above. As a result, the new arcminute-resolution image of the Orion region has an rms noise of 5 mJy beam^{-1}. The imaging sensitivity is thus improved by a factor of 2. The new image better represents the extended emission associated with the H II regions M42 and M43. In addition, the new image covers a wide field that includes the NGC 1973-75-77 nebulae located about half a degree to the north.

A contour representation of the new wide-field VLA 330 MHz image of the Orion region, made with a beam of 79×65 arcsec^2, is shown in Figure 1. The radio contours have been overlaid on a UKS008 deep image (discussed below in § 2.1) of the Orion region made with the UK Schmidt telescope. We show in Figure 2 details of the radio morphology in M42 as a contour representation that is overlaid on a black and white version of the UK Schmidt optical picture. The wide field covers the sky region that appears to the unaided eye as the sword of Orion: the M42 and M43 nebulosities in the center of Figure 1 appear as the central "star" in the sword, the NGC 1973-75-77 nebulosities to the north appear as the northern "star."

The extended optical nebulosity at the center of Figure 1 comprises the extended asymmetric radio H II region M42

and the symmetric H II region M43, which is located about 8' to the north of the peak of M42 and appears in the radio as a distinct "head." In comparison with the earlier image in Subrahmanyan (1992), the present image better reproduces the extended emission in M42. In particular, radio emission is now detected farther south by almost 10'. After corrections for the primary beam attenuation, we integrate the flux density over the source regions and estimate the total flux density of M42 and M43 to be 155 ± 5 and 12 ± 1 Jy, respectively. The peak flux density toward M42 is 3.3 Jy beam^{-1}, and that toward M43 is 1.7 Jy beam^{-1} in the image made with a beam of 79×65 arcsec^2.

The beam-averaged brightness temperature toward the continuum peak of M42 is 7160 K. As discussed in Subrahmanyan (1992), the high free-free opacity toward the continuum peak at 330 MHz makes the brightness temperature at this frequency a good estimate of the physical electron temperature in the thermal ionized plasma along the line of sight. It may be noted here that the peak brightness—corrected for (1) possible dilution due to the finite beam, (2) background brightness that is missing in the Fourier synthesis imaging, and (3) finite opacity—was used by Subrahmanyan (1992) to derive an estimate of 7865 ± 360 K for the electron temperature toward M42.

There are several radio images of the large-scale (exceeding a few arcminutes) radio structure of Orion A in the literature; however, the 330 MHz image presented here has detected more extensive emission surrounding M42 than any previous image of the region. Most remarkable is the detection of the low surface brightness emission extending toward the south and west.

In Figure 3 we show a north-south profile across the VLA 330 MHz image of the radio nebula, made along R.A. $05^h 35^m 27^s$ (J2000.0). The profile cuts across M42 and M43, which are seen as distinct intense peaks at $\approx 0''$ and $+450''$, respectively. The profile plotted has been clipped at 1 Jy beam^{-1} flux density to show clearly the separate low surface brightness halo component that is visible in the figure extending south from about -0.4 kiloarcsec to at least -1.2 kiloarcsec from the peak of M42.

The halo component is more readily imaged at low radio frequencies, e.g., 330 MHz, because the central regions with high emission measure are optically thick at low frequencies and the contrast between the bright center and diffuse halo is reduced toward lower radio frequencies. Consequently, detection of the halo component would require lower dynamic range imaging at lower frequencies. Any halo component that has a nonthermal spectrum would also be more easily visible in low-frequency images.

We detect extended radio continuum emission from NGC 1977. Confirming the 6 cm radio continuum observations of Kutner et al. (1985), we find a peak in the 330 MHz continuum in the southern end of this source that is coincident with a bright rim in the optical continuum. The double radio source seen in the southeastern part of NGC 1977 is probably an extragalactic radio source seen as a chance superposition on the nebulosity.

2.1. UKS008 Optical Image of the Orion Nebula

The optical color image (Fig. 1) was constructed by David Malin using unsharp masking (Malin 1977) by combining three separate 60 minute–exposure black and white plates that were made using emulsion/filters IIa-O/GG 385, IIa-D/GG 495, and 098-04/RG 630.
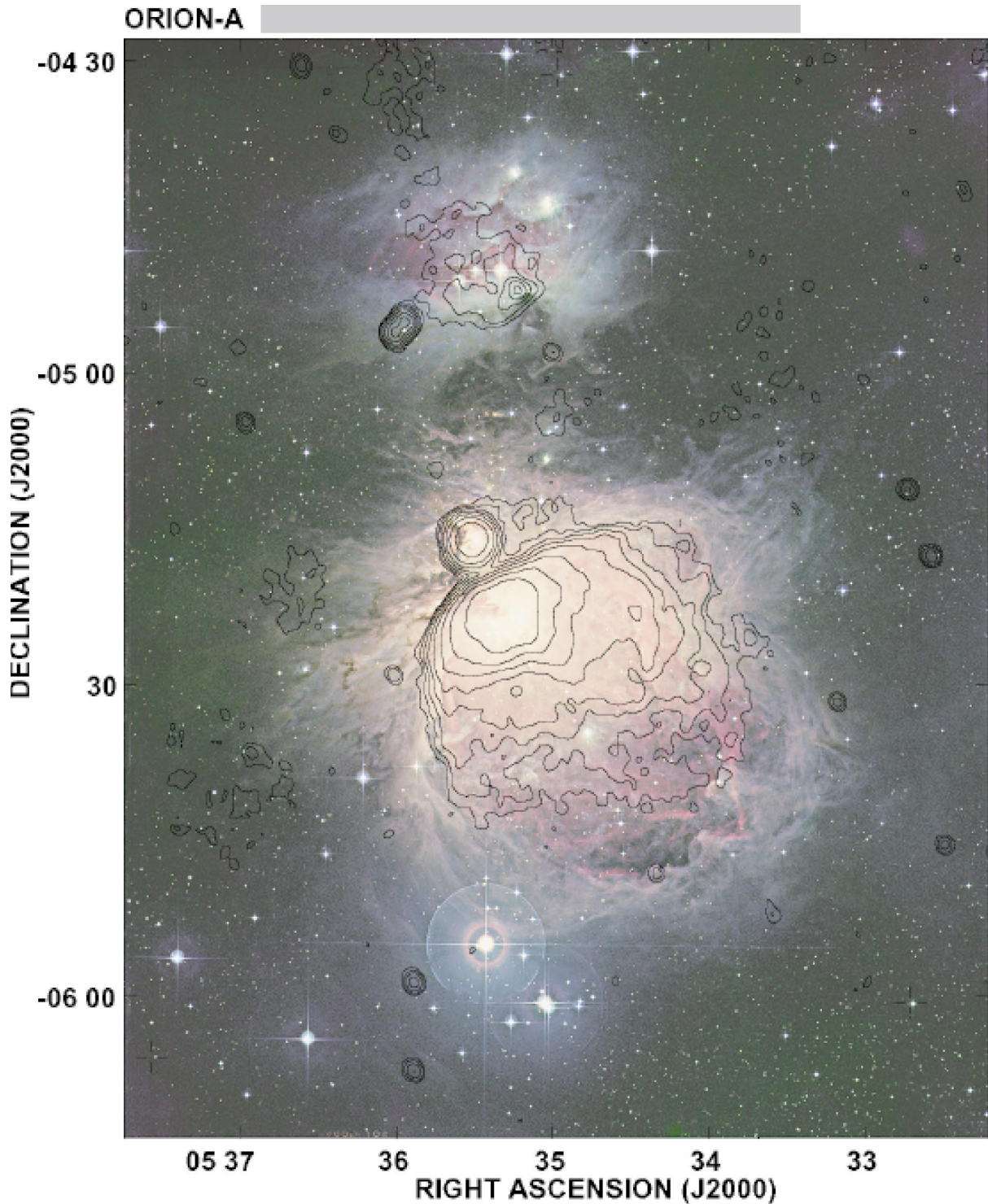
FIG. 1.—Overlay of the VLA 330 MHz radio contours on a UK Schmidt optical photograph of the Orion region. The bright dominant nebulosity at the image center is M42, the relatively smaller nebulosity located just beyond the northeastern rim of this nebula is M43, and the separate nebulosity located to the north is NGC 1973-75-77. Radio contours are at 1, 2, 4, 8, 16, 32, 64, 128, and 256 times 15 mJy beam^{-1}. The radio image was made with a beam of 79×65 arcsec^2 at P.A. 25°.

The deep optical image of M42 indicates two distinct color components in the nebula. The intense yellowish nebula immediately surrounding the Trapezium stars represents predominantly green and red line radiation from oxygen and hydrogen in higher temperature H II gas. The red colors arise because of the Balmer alpha line of hydrogen (Hα), and the green is a mix of [O III] λ4959, [O III] λ5007, and higher order transitions of the hydrogen Balmer series. This centrally condensed nebulosity is brightest close to the exciting stars and appears to be sharply bounded along a curved rim in the northeast. A mauve filamentary shell appears to envelop the redder nebula. Toward the southwest, these bluer filaments appear to form an extensive loop or shell. These shell-like filamentary structures are seen in Figure 2 at bottom right, passing through R.A. 05^{h}33^{m}30^s, decl. $-05°40'$ (J2000.0).
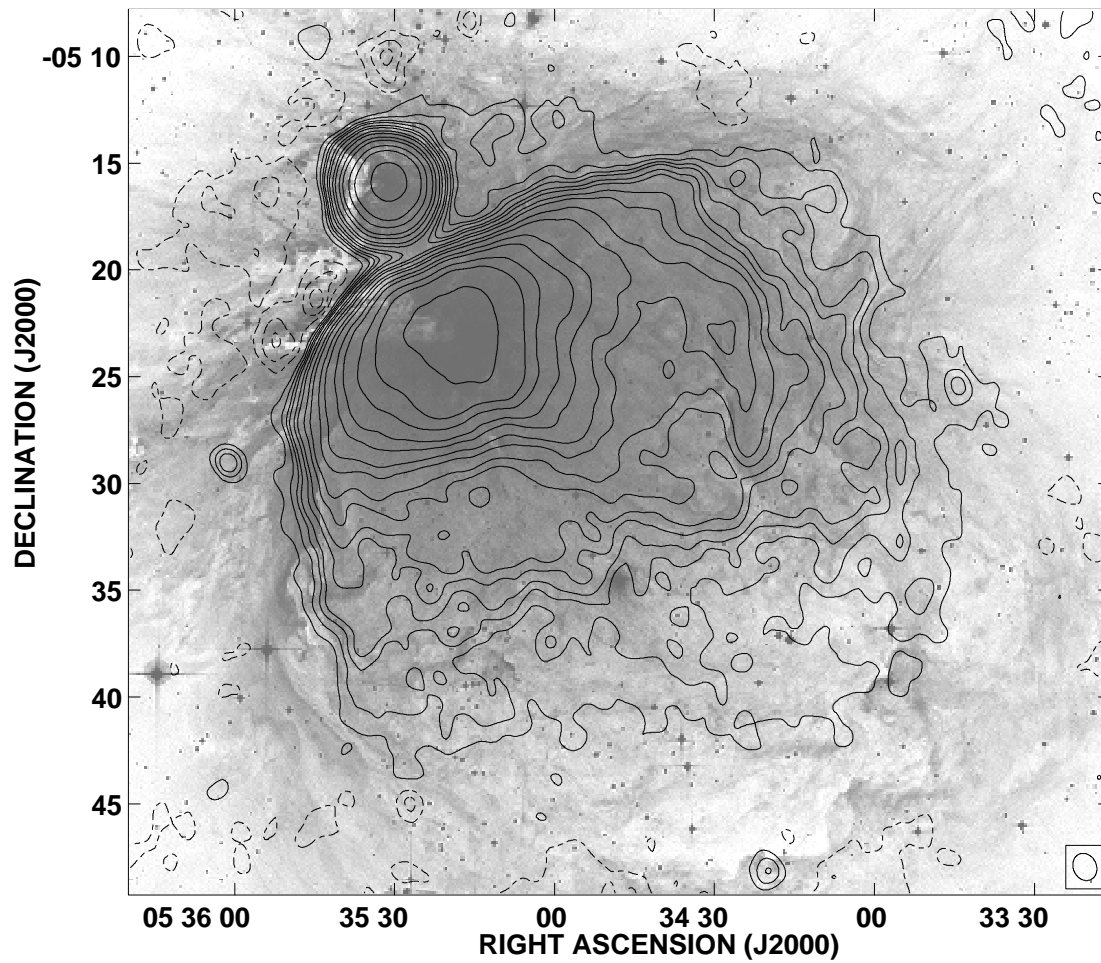
FIG. 2.—M42 and M43 H II regions: 330 MHz VLA radio contours overlaid on a gray-scale representation of the UK Schmidt optical image of the region. The radio image was made with a beam of 79×65 arcsec^2 at position angle P.A. 25°. Contours are at -4, -3, -2, -1, 1, 2, 3, 4, 6, 8, 12, 16, 24, 48, 64, 96, 128, and 192 times 15 mJy beam^{-1}. The image has been corrected for the primary beam attenuation.
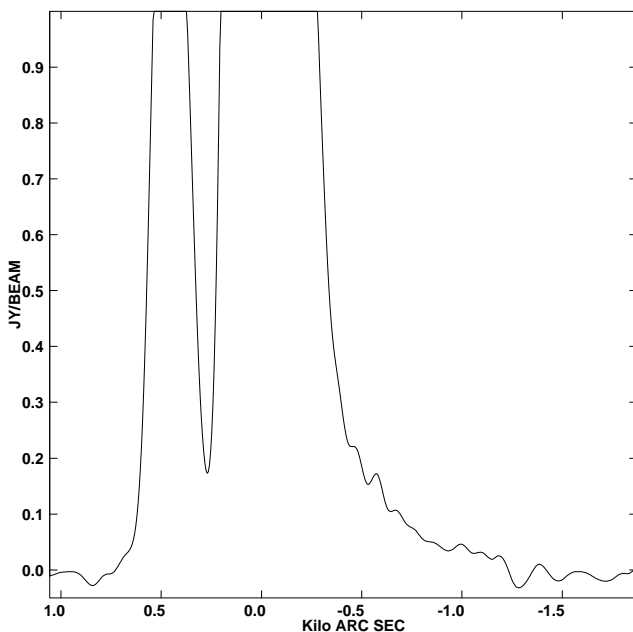

FIG. 3.—Slice through the VLA 330 MHz image of the region along RA 05^{h}35^{m}27^s (J2000.0).

3. COMPARISON WITH A 1.5 GHz RADIO IMAGE OF ORION A

A VLA 1.5 GHz image of Orion A, comprising M42 and M43, was made by Yusef-Zadeh (1990). We have used part of his data, which were obtained in the most compact D array configuration of the VLA, to make a low-resolution image of Orion A. We show, in Figure 4, this continuum image at 1.5 GHz with a beam of 1′ FWHM. The diffuse emission has been detected, in the 1.5 GHz image, extending 7′ south of the peak of M42. In comparison, the 330 MHz image has been vastly superior in imaging the extended low surface brightness emission: it has successfully imaged the emission to extend at least 20′ to the south of the peak of M42.

We have convolved both continuum images to a common resolution of 80″ and computed the distribution of spectral index over the regions that have been imaged at both frequencies. It may be noted here that the 1.5 GHz image was constructed using data from the VLA D array, whereas the 330 MHz image was made using data from the VLA DnC hybrid and D arrays: the 1.5 GHz image is not expected to reproduce successfully all the large-scale structures that may be seen in the 330 MHz image. The spectral
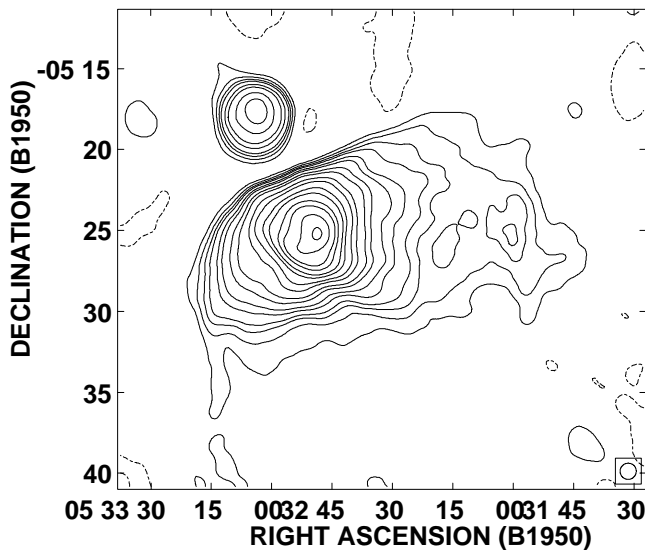
FIG. 4.—VLA 1.5 GHz image of the Orion region made with a beam of 1′ FWHM. Contours are at −0.1, 0.1, 0.2, 0.3, 0.4, 0.6, 0.8, 1.2, 1.6, 2.4, 3.2, 4.8, 6.4, 9.6, 12.8, 19.2, 25.6, and 38.4 Jy beam^{-1}. The image has been corrected for the primary beam attenuation.

index image is shown in Figure 5 (we adopt the definition $S_\nu \sim \nu^\alpha$ for the spectral index, α). Toward the peak of M42 the spectral index, computed between 330 MHz and 1.5 GHz, is about 1.6. Away from the peak, the opacity drops, and the spectral index $\alpha \approx 0.1$ at a distance of 4′ from the peak. Outside this central region the opacity is fairly uniform at $\alpha \approx 0 \pm 0.1$ and is consistent, within the errors in the measurements, with optically thin thermal bremsstrahlung emission. There is no sign of any nonthermal emission in the spectral index image. The low-frequency turnover in the spectrum toward the central regions of M42 is due to free-free absorption. The spectral index toward the continuum peak in M43 is about 0.3, as computed between 330 MHz and 1.5 GHz.
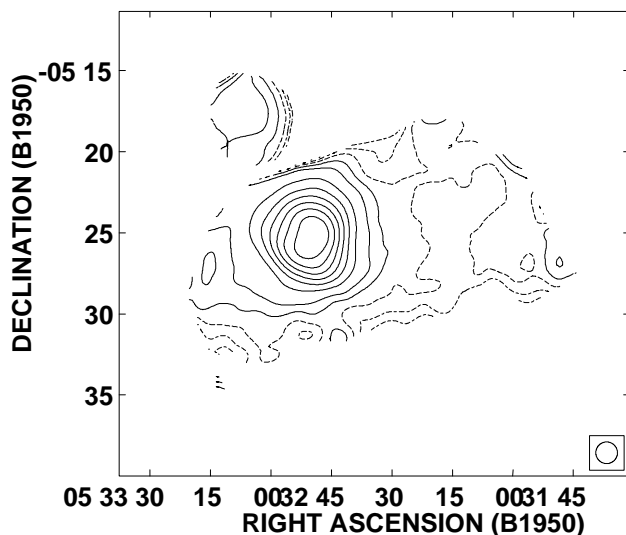

FIG. 5.—Distribution of spectral index as computed between 330 MHz and 1.5 GHz (we adopt the definition $S_\nu \sim \nu^\alpha$ for the spectral index, α). The image resolution is 80″ FWHM, and the peak spectral index is 1.6. Contours are at −0.2, −0.1, 0.0, 0.1, 0.2, 0.4, 0.6, 0.8, 1.0, 1.2, and 1.4′. Dashed lines show negative contours and the zero-level contour.

The extended emission surrounding M42 appears to have a distinct, curved, partial shell-like component located 12′ to the west of the main peak. This feature is not as sharply bounded as the emission edge on the northeastern side of the peak. The structure is seen in the 330 MHz and 1.5 GHz images, and its spectral index is close to zero, indicating that it is an optically thin thermal emission component. It may be noted here that this western component also appears in the 408 MHz image in Mills & Shaver (1968) and is detected in the 5 GHz image of Goss & Shaver (1970).

4. RADIO IMAGE OF M42 AND M43 AT 10.55 GHz

We have imaged Orion A using the four-feed 10.55 GHz receiver (Schmidt et al. 1993) on the Effelsberg 100 m telescope in 1994 September. The four beams are separated only in azimuth, and the Orion region was scanned by moving the telescope in azimuth and observing the source row by row. Orion A was observed around meridian crossing while the source parallactic angle changed by about 35°. During this period, two sets of scans were completed, and a sky region of about 45′ in east-west and 40′ in north-south was covered by the 45′ long scans, which were separated by 1′.

The image of Orion A was constructed using only difference measurements between horn pairs; these are relatively insensitive to atmospheric effects (Emerson, Klein, & Haslam 1979). The image was deconvolved using a model beam pattern rotated to the mean parallactic angle of the observations. Unfortunately, during our observations, the Effelsberg telescope azimuthal drive suffered from pointing errors owing to hysteresis. The magnitude of the hysteresis was estimated using the scans on the calibrator, and the scans on Orion A were corrected by offsetting alternate scans. The relative horn gains and the telescope pointing were determined by observing the unresolved calibrator 3C161 in a similar raster-scanning mode. The 10.55 GHz flux density of this calibrator, on the scale of Baars et al. (1977), is 2.94 Jy (Ott et al. 1994), and the amplitude of the scans over 3C161 were used to set the absolute flux scale in the imaging. The image resolution was also determined by fitting a two-dimensional Gaussian to the scans over the calibrator. The absolute coordinate reference frame was refined by aligning the position of the peak of M43 in the 10.55 GHz image to the corresponding peak in the 1.5 GHz image. For this alignment both images were convolved to a common resolution.

A contour representation of the image, smoothed to a resolution of 90″ FWHM, is shown in Figure 6. It may be noted here that, because the four beams are separated in azimuth and because the quadrupod supporting the subreflector causes higher antenna sidelobes in the azimuthal plane, the image is dynamic-range limited, particularly in the east-west scans through the bright emission peak of M42. Consequently, the 10.55 GHz image has artifacts to the east and west of the emission peak and may have spurious "excess" flux density along this line. The image is more reliable away from the east-west line through the peak and has successfully detected the extended low surface brightness emission in the south of M42. Although the image quality is not as good, the halo emission detected in the 10.55 GHz image is almost as extensive as the halo detected in the VLA 330 MHz image: this confirms the existence of the radio continuum halo.
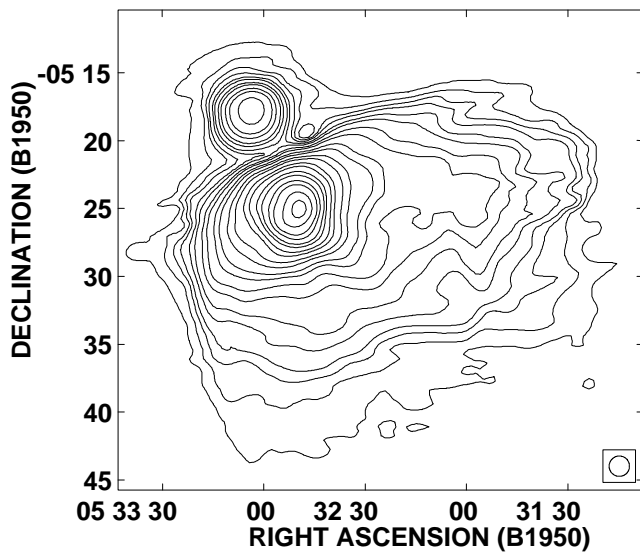
FIG. 6.—10.55 GHz Effelsberg image of Orion A made with a beam of 90″ FWHM. Contours are at 1, 2, 3, 4, 6, 8, 12, 16, 24, 32, 48, 64, 96, 128, 192, 256, 384, 512, 768, and 1024 times 50 mJy beam^{-1}.

In Figure 7, we show the distribution of spectral index, computed between 330 MHz and 10.55 GHz, over Orion A. The spectral index toward the peak of M42 is 0.7. At the resolution of 90″ the spectral index flattens to 0″.1 about 3″.5 away from the peak. We ignore the region to the extreme west of M42 because of possible artifacts in this region, as discussed above. An extended region, located about 7′ to the south of the peak of M42, appears as a broad patch that has a relatively flatter spectral index in the range 0.2–0.1.

5. RADIO HALO IN M42: RELATIONSHIP TO OPTICAL STRUCTURES

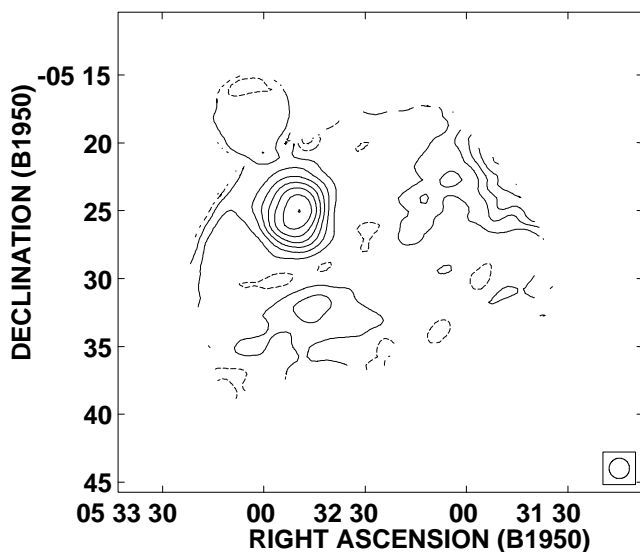The spectral index images presented above indicate that the halo component is optically thin thermal bremsstrah-

FIG. 7.—Distribution of spectral index as computed between 330 MHz and 10.55 GHz. The image resolution is 90″ FWHM, and the peak spectral index is 0.7. Contours are at −0.1, 0.0, 0.1, 0.2, 0.3, 0.4, 0.5, 0.6, and 0.7′. Dashed lines show the negative and zero contours.

lung emission: this is the case for the western component as well as the southern extension. There is no evidence that any part of the halo we detect is nonthermal.

The radio halo in M42, seen in Figure 1 overlaid with the optical picture of the nebula, appears coincident with the yellowish part of the optical nebulosity. The radio emission peaks in the vicinity of the Trapezium exciting stars, and, like the optical image, the radio intensity is sharply bounded along the same curved rim to the northeast. The radio surface brightness progressively diminishes toward the south and west, and the radio structure appears to terminate to the southwest in a pair of pincer-like structures. These radio wisps coincide with similar optical arcs that, in turn, represent the southwestern end of the redder structure. To summarize, it appears that the radio morphology is similar to and demarcates the redder parts of the optical nebulosity.

The radio emission has been shown to be wholly thermal free-free bremsstrahlung and represents H II gas. The redder parts of the optical nebula, which are also expected to represent H II gas, are—consistent with expectation—detected in the radio continuum. The bluish color in the filamentary features at the periphery of the nebula are believed to be indicative of reflection nebulosity due to scattered light from OB stars. Consistent once again with expectations, the mauve filaments are undetected in radio continuum. On the other hand, it is possible that H II gas present in the filamentary structures have a lower emission measure and, therefore, have been undetected in the present observations. Nevertheless, we may conclude that we find no evidence for radio continuum emission from optical structures outside the redder H II regions where Hα predominates. Our observations are consistent with these optical filaments being reflection nebulosity.

Toward the peak of M42, the 10.55 GHz image made with a beam of 90″ FWHM has flux density 51 Jy beam^{-1}. The electron temperature of the thermal plasma was estimated to be 7865 K, based on the brightness toward the opaque continuum peak in the 330 MHz image; this estimate is consistent with other estimates based on optical emission lines, optical continuum measurements, and radio recombination lines (see, for example, Goudis 1982; Subrahmanyan 1992). Adopting this value for the electron temperature, we derive the emission measure toward the continuum peak to be 2.7×10^6 pc cm^{-6}. The optical recombination line intensity from a thermal gaseous nebula is expected to be given by

$$\int I_v \, dv = 2.46 \times 10^{17} h v \alpha_{mn} \, EM \, , \tag{1}$$

where h is Planck's constant, v is the optical line frequency (in hertz), EM is the emission measure in pc cm^{-6}, and α_{mn} is the photon production coefficient in cm^3 s^{-1} (Spitzer 1978). Adopting a value of $\alpha_{32} = 14 \times 10^{-14}$ cm^3 s^{-1} for the Hα photon production rate, we expect the Hα line intensity toward the peak of M42 to be 0.3 ergs cm^{-2} sr^{-1} s^{-1}, assuming no internal or external absorption by dust. The observed Hα intensity toward this direction is 0.15 erg cm^{-2} sr^{-1} s^{-1} (Schmitter 1971) and is within a factor of 2 of the prediction based on the radio continuum intensity. It may be noted here that, more recently, O'Dell & Yusef-Zadeh (2000) have compared the radio continuum with the Hα and Hα–Hβ line ratios toward the central parts of the M42 nebula with high angular resolution.

Toward the mauve optical filaments, we place a 2 σ upper limit of 10 mJy beam^{-1} on the 330 MHz flux density, based on our radio image made with a beam of 1.2 FWHM. Adopting the same assumptions stated above, we estimate that the emission measure of any H II gas toward these filaments is less than about 600 pc cm^{-6}. The corresponding Hα optical recombination radiation from these regions is, consequently, expected to be less than 6×10^{-5} erg cm^{-2} sr^{-1} s^{-1}. Our deep optical image of the filamentary nebulosity does not have an accurate intensity scale; however, the brightness of the mauve filaments certainly exceeds 23 mag arcsec^{-2}.

To conclude, the optical emission and radio continuum brightness toward the continuum peak are in agreement with the hypothesis that both are attributable to emission from thermal gas; however, toward the mauve filaments, the optical emission is brighter than that expected based on the radio continuum. This is consistent with our interpretation of the outermost mauve filaments as being predominantly reflection nebulosity. A conclusive resolution of the problem would be aided by a quantitative measure of the optical Hα intensity toward these outer filaments.

The 330 MHz VLA radio image has detected an extended thermal halo around M42; however, the extent of the halo appears confined to the optically redder regions of the nebulosity. We see no evidence that the H II gas associated with the H II region extends farther where the optical emission appears to be bluer. The halo we detect corresponds to a structure with a maximum size of about 6 pc and, assuming an electron temperature of 5000 K, has an emission measure of about 5000 pc cm^{-6} and an electron density of about 30 cm^{-3}. If, as suggested by Anantharamaiah (1986), Kassim (1989), and Roshi & Anantharamaiah (2000), low-density envelopes with electron density $n_e \sim$ 0.5–10.0 cm^{-3} and size 50–200 pc exist surrounding H II regions, our 330 MHz image has failed to detect one in M42. We see no evidence for a "transition" H II component between the higher density H II region and the warm ionized medium of the ISM.

It may be noted here that we do not believe there is any flux density missing in our 330 MHz VLA image. The total flux density of the Orion Nebula has been estimated, from single-dish measurements, to be 124 Jy at 234 MHz (Terzian, Mezger, & Schraml 1968) and 213 Jy at 408 MHz (Mills & Shaver 1968): the total flux density of M42 and M43 in our 330 MHz VLA image is 167 $\pm$ 6 Jy, close to the expectation based on these earlier estimates.

6. H II REGION NGC 1977

NGC 1977 has been studied in the literature because it has been recognized to have an H II region–molecular cloud interface that is nearly edge-on. Extended radio continuum emission with a source size about 5'—representing the H II gas—was detected in NGC 1977 at 5 GHz (Goss & Shaver 1970) with a total continuum flux density of 1.8 Jy (Shaver & Goss 1970). CO line emission from the associated molecular cloud to the south (Kutner, Evans, & Tucker 1976) suggested the presence of a shock front in the molecular gas that presumably precedes the ionization front. Kutner (1979) detected C110α and C76α carbon recombination lines, confirming the presence of a distinct boundary region at a transition between H II and molecular gas.

The optical nebulosities NGC 1973-74-77 are believed to be primarily reflection nebulae surrounding an open star cluster. Part of the optical intensity seen toward the southernmost part of these nebulae is yellowish, in discordance with other reflection nebulae that are blue; this is explained as attributable to the reflection of light originating in the bright core of the greater Orion Nebula to the south (see, for example, Malin 1993).

In Figure 8, we show 330 MHz radio contours of NGC 1977 overlaid on a gray-scale image of the optical nebula. The total flux density of the source is estimated to be 3.6 Jy at 330 MHz. The radio source may be decomposed into two components: an extended source that appears edge-brightened toward the southwestern end and a compact unresolved source that is located at the southwestern edge of the extended radio source. The edge-brightened ridge presumably delineates the ionization-bounded limit of the H II gas at the interface with the molecular cloud. This ridge has been imaged with greater clarity by Kutner et al. (1985) at 5 GHz. Excluding the compact source, we estimate the spectral index of the extended component to be about -0.2: within the errors we infer that the extended source is an optically thin thermal H II region at 330 MHz.

The detection of H II gas in radio continuum in the southern parts of NGC 1977 suggests that at least part of the optical light from these parts of the nebula may represent emission nebulosity: the entire optical nebula is unlikely to be a reflection nebulosity. As was the case in M42, the 330 MHz extended radio continuum in NGC 1977 is brighter in the redder parts of the nebula.

6.1. Compact Source in NGC 1977

The emission peak seen within the extended radio structure of NGC 1977 (not to be confused with the brighter double radio source located to the southeast and outside the radio nebula), in the 330 MHz image shown in Figure 8, is located close to the H II molecular cloud interface and is also coincident with the bright optical rim that forms a sharp boundary south of the nebula. The compact source was observed previously in a VLA 5 GHz image of NGC 1977 by Kutner et al. (1985) who argue, based on the absence of 2 μm emission, against it being either a separate compact H II region or a dense clump of gas.

Apart from the 330 MHz image, we have observed the compact source at 1420, 4860, and 8440 MHz with the VLA: we estimate the flux density of the compact component to be 320, 50, 11.4, and 5.2 mJy at 330, 1420, 4860, and 8440 MHz, respectively. The spectrum of the component is straight and steep over this range of frequencies, and the spectral index α is about -1.3; there is no evidence for any spectral break or turnover down to 330 MHz. The 8440 MHz VLA observations were made with the VLA in the A array with a synthesized beam of 200 mas, and the source appeared unresolved; we estimate its angular size to be less than 100 mas. The compact object is located at R.A. $05^h35^m13^s.680$, decl. $-04°52'01''.96$ (J2000.0). The spectrum and brightness indicate that the compact component is a nonthermal synchrotron source.

If the compact source is a Galactic pulsar located in the vicinity of NGC 1977 and about 0.5 kpc from the Sun, its flux density would be unusually high. An attempt to detect radio pulsations at 330 MHz was unsuccessful (R. Ramachandran 1995, private communication); however, if the object is embedded in or is behind the H II region in NGC 1977, the high dispersion measure may make the detection of pulsed emission difficult.
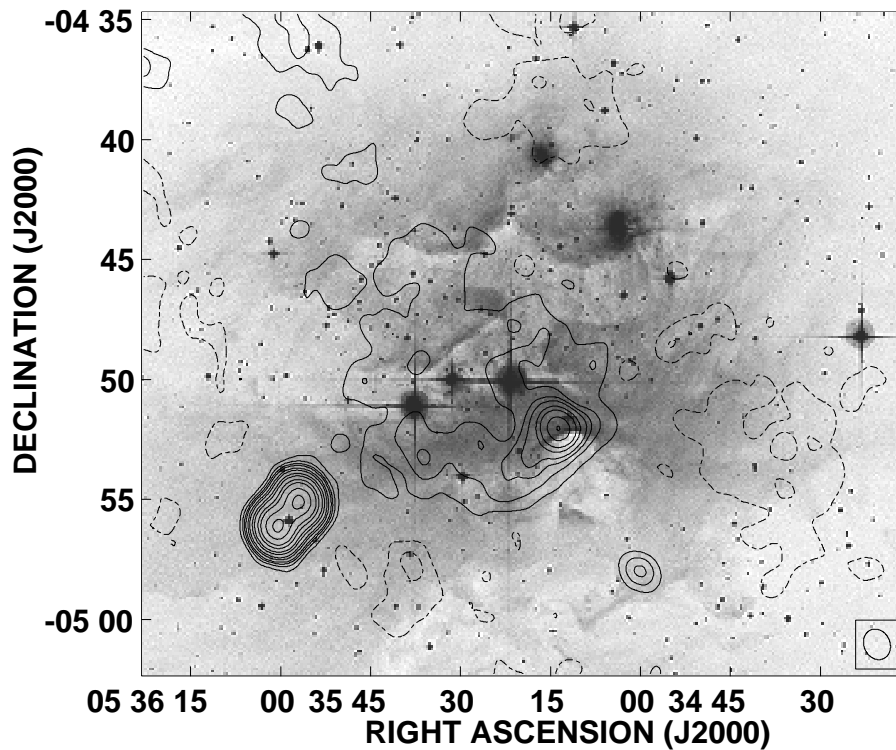
FIG. 8.—NGC 1977 H II region: 330 MHz radio contours overlaid on a gray-scale image of the optical nebula. The compact source discussed in § 6.1 is the radio peak embedded in the extended radio emission at the center of the image; the peak is seen to be coincident with a bright optical rim. The double radio source in the southeastern part of the image is an unrelated extragalactic source. The radio image has been made with a beam of 79×65 arcsec^2 at position angle P.A. 25°. Contours are at $-2, -1, 1, 2, 3, 4, 6, 8, 12, 16, 24, 48, 64$, and 96 times 20 mJy beam^{-1}. The image has been corrected for the primary beam attenuation.

The double radio source seen to the southeast in Figure 8 is extragalactic: VLA imaging at 1.4 GHz reveals a core with symmetric edge-brightened lobes typical of Fanaroff-Riley Type II radio galaxies. Toward this extragalactic source, multiple H I absorption features are seen over the LSR velocity range 2–20 km s^{-1}. Along the line of sight toward the compact source in NGC 1977, H I absorption is observed in the range 5–24 km s^{-1}. It may be noted here that the CO molecular transitions and carbon recombination lines in NGC 1977 have been detected in emission with LSR velocities about 12 km s^{-1}. The relative strengths of the H I absorption features differ toward the two sources, but there is no compelling evidence from the absorption to suggest that the compact steep-spectrum source in NGC 1977 is Galactic.

The emission measure of the H II region along the line of sight toward the compact source is about 5000 pc cm^{-6}. If the compact source is located behind the H II gas, we may expect scattering effects in the plasma to manifest in an angular broadening and possibly temporal variability in the flux density of the compact source. A scatter-broadened source is expected to have an angular size that scales approximately as the square of the observing wavelength, and multifrequency measurements of the source size may shed light on the relative locations along the line of sight of the compact and extended emission in NGC 1977.

The radio continuum image at 330 MHz was made with the VLA of the National Radio Astronomy Observatory, a facility of the National Science Foundation operated under cooperative agreement by Associated Universities, Inc. We thank R. Wielebinski for his support, K.-H. Mack for assistance with the Effelsberg observing, Farad Yusef-Zadeh for the VLA 20 cm D array data, Patrica Reich for assistance with the NOD2 software, and K. R. Anantharamaiah for his comments on an earlier version of the manuscript.

REFERENCES

Anantharamaiah, K. R. 1985, J. Astrophys. Astron., 6, 203
———. 1986, J. Astrophys. Astron., 7, 131
Baars, J. W. M., Genzel, R., Pauliny-Toth, I. I. K., & Witzel, A. 1977, A&A, 61, 99
Emerson, D. T., Klein, U., & Haslam, C. G. T. 1979, A&A, 76, 92
Goss, W. M., & Shaver, P. A. 1970, Australian J. Phys. Astrophys. Suppl., 14, 1
Goudis, C. 1982, Astrophys. Space Sci. Libr., 90, 100
Kassim, N. E. 1989, ApJ, 347, 915
Kulkarni, S. R., & Heiles, C. 1987, in Interstellar Processes, ed. D. J. Hollenbach & H. A. Thronson (Dordrecht: Reidel), 87
Kutner, R. L. 1979, ApJS, 40, 1
Kutner, M. L., Evans, N. J., II, & Tucker, K. D. 1976, ApJ, 209, 452
Kutner, M. L., Machnik, D. E., Mead, K. N., & Evans, N. J., II. 1985, ApJ, 299, 351

Lockman, F. J. 1980, in Radio Recombination Lines, ed. P. A. Shaver (Dordrecht: Reidel), 185
Malin, D. F. 1977, AAS Photo Bull., No. 16, 10
———. 1993, A View of the Universe (Cambridge: Cambridge Univ. Press)
McKee, F., & Williams J. P. 1997, ApJ, 476, 144
Mezger, P. G. 1978, A&A, 70, 565
Mills, B. Y., & Shaver, P. A. 1968, Australian J. Phys., 21, 95
Murdin, P. G., Allen, D. A., & Malin, D. 1979, in A Catalogue of the Universe, ed. P. Murdin (Cambridge: Cambridge Univ. Press)
Napier, P. J., Thompson, A. R., & Ekers, R. D. 1983, Proc. IEEE, 71, 1295
O'Dell, C. R., & Yusef-Zadeh, F. 2000, AJ, 120, 382
Ott, M., Witzel, A., Quirrenbach, A., Krichbaum, T. P., Standke, K. J., Schalinski, C. J., & Hummel, C. A. 1994, A&A, 284, 331
Peimbert, M. 1982, in Ann. NY Acad. Sci., 395, Symposium on the Orion Nebula, ed. A. E. Glassgold, P. J. Huggins, & E. L. Schucking, 24

Roshi, D. A., & Anantharamaiah, K. R. 2000, ApJ, 535, 231
Schmidt, A., Wongsowijoto, S., Lochner, O., Reich, W., Reich, P., Fürst, E., & Wielebinski, R. 1993, technisher bericht des MPIfR, Bonn, No. 73
Schmitter, E. F. 1971, AJ, 76, 571
Shaver, P. A., & Goss, W. M. 1970, Australian J. Phys. Astrophys. Suppl., 14, 133
Smith, L. F., Biermann, P., & Mezger, P. G. 1978, A&A, 66, 65

Spitzer, L. A., Jr. 1978, Physical Processes in the Interstellar Medium (New York: Wiley)
Subrahmanyan, R. 1992, MNRAS, 254, 291
Terzian, Y., Mezger, P. G., & Schraml, J. 1968, Astrophys. Lett., 1, 153
Van der Werf, P. P., & Goss, W. M. 1989, A&A, 224, 209
Yusef-Zadeh, F. 1990, ApJ, 361, L19